

## Anomalous Discontinuity at the Percolation Critical Point of Active Gels

M. Sheinman,<sup>1,2</sup> A. Sharma,<sup>1</sup> J. Alvarado,<sup>3,4</sup> G. H. Koenderink,<sup>3</sup> and F. C. MacKintosh<sup>1</sup>

<sup>1</sup>*Department of Physics and Astronomy, VU University, 1081 HV Amsterdam, Netherlands*

<sup>2</sup>*Max Planck Institute for Molecular Genetics, 14195 Berlin, Germany*

<sup>3</sup>*FOM Institute AMOLF, Science Park 104, 1098 XG Amsterdam, Netherlands*

<sup>4</sup>*Department of Mechanical Engineering, Hatsopoulos Microfluids Laboratory, Massachusetts Institute of Technology, Cambridge, Massachusetts 02139, USA*

(Received 9 January 2015; published 4 March 2015)

We develop a percolation model motivated by recent experimental studies of gels with active network remodeling by molecular motors. This remodeling was found to lead to a critical state reminiscent of random percolation (RP), but with a cluster distribution inconsistent with RP. Our model not only can account for these experiments, but also exhibits an unusual type of mixed phase transition: We find that the transition is characterized by signatures of criticality, but with a discontinuity in the order parameter.

DOI: [10.1103/PhysRevLett.114.098104](https://doi.org/10.1103/PhysRevLett.114.098104)

PACS numbers: 87.16.Ka, 64.60.ah, 64.60.Bd, 64.60.De

Percolation theory has become pervasive in a number of fields ranging from physics to mathematics and even computer science [1]. In particular, it successfully describes connectivity and elastic properties of polymer networks [2,3]. The simplest percolation model is the random percolation (RP) model, consisting of a collection of nodes with controlled connectivity,  $p$ , representing the fraction of occupied bonds between the nodes. As a function of  $p$ , the order parameter—the mass fraction of the largest cluster—becomes finite above the percolation threshold  $p_c$ . The nature of the transition is of special interest because the system properties are highly tunable at this point, especially if the transition is discontinuous; in that case, just a few bonds can have a significant impact, even for very large systems [4]. Usually, however, percolation transitions are second order, with a continuous variation of the order parameter and various critical signatures. More specialized percolation models can exhibit different phase behavior, including discontinuous transitions between the two phases (see discussion below).

Here, we present a simple model based on random percolation that develops a discontinuous jump in the order parameter in the thermodynamic limit, while exhibiting other features of criticality in such quantities as the correlation length and susceptibility. Interestingly, the transition we observe occurs for the same  $p_c < 1$  as for random percolation. Moreover, our model can account for recent experimental results on active biopolymer gels that have been shown to self-organize towards a critical connectivity point [5]. The experimentally observed cluster properties at this point were found to be inconsistent with the ordinary random percolation model.

In these experiments, we studied a model cytoskeletal system, composed of actin filaments, fascin cross-links and myosin motors in a quasi-2D chamber of dimensions  $3\text{ mm} \times 2\text{ mm} \times 80\text{ }\mu\text{m}$  [5] (see Supplemental Material [6]). We observed a motor-driven collapse of the network into

disjointed clusters (see Fig. 1(a) and movie of the collapse in the Supplemental Material [6]). The configuration of the clusters prior to the collapse is obtained by analyzing the time-reversed movie [see Fig. 1(b)] and their masses were estimated from their initial areas. We found that, over a wide range of the experimental parameters, the number  $n_s$  of clusters of mass  $s$  exhibits a power-law distribution:  $n_s \sim s^{-\tau}$ . Here,  $\tau$  is the Fisher power-law exponent, which must be strictly limited to values  $\geq 2$  for the RP model [7]. It was found experimentally, however, that  $\tau \approx 1.91 \pm 0.06$ . A key feature of these experiments is the apparent absence of enclaves—clusters fully surrounded by another cluster [see inset of Fig. 1(c)]. These enclaves are responsible for the fractal nature of clusters and  $\tau > 2$  in the RP model [8,9]. Below, we show that the, apparently paradoxical, experimental features of  $n_s \sim s^{-\tau}$ , yet with  $\tau < 2$  can be understood within our no-enclaves percolation (NEP) model.

*NEP model and its theoretical analysis.*—Our NEP model begins with the random percolation model, but in which enclaves—clusters fully surrounded by a larger cluster—are absorbed into the surrounding cluster (see Figs. 1(c), 2(a) and Supplemental Material [6]). We do this because, in the experiments, during the collapse, as a single connected cluster contracts, it tends to incorporate other material within the cluster, including distinct enclaves contained within it (see illustration in the Supplemental Material [6]). Thus, experimentally the final cluster configuration, obtained from the time-reversed movie, is enclave free [see Fig. 1(b)]. In the NEP model, as in the RP model, massive nodes are located on a regular lattice. Nearest-neighbor nodes are connected by massless bonds with a probability  $p$ . For any  $p$ , the total system mass (in units of nodes) is equal to the total number of nodes,  $M$ . For a given value of  $p$ , the network is obtained from the corresponding network of the RP model, but with all enclaves absorbed into their surrounding clusters (they can also be absorbed during each step of the dilution

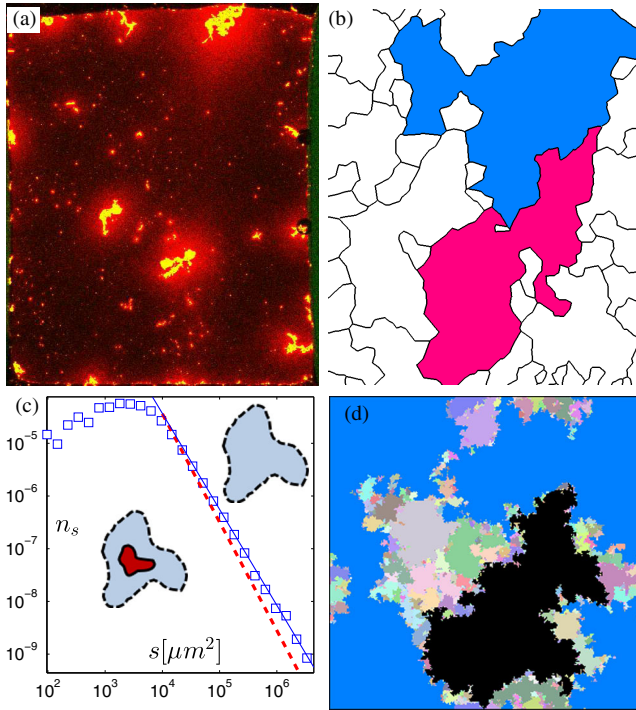


FIG. 1 (color online). (a) Experimental results of a fascin-crosslinked actin network, collapsed by myosin motors (see Supplemental Material [6] for details and movie of the collapse). (b) Initial configuration of the collapsed clusters in (a). Colors indicate the largest (blue) and the second-largest (pink) clusters. (c) Histogram (squares) of cluster masses, averaged over 26 samples. For the critically connected regime, the data are statistically more consistent (1.4 standard errors from the Hill estimator of  $\tau = 1.91 \pm 0.06$  [10]) with a power-law distribution with a NEP model's Fisher exponent from Eq. (9) (solid line). The agreement of the data with the RP model Fisher exponent  $\tau' = 187/91$ , indicated by the dashed line, is significantly worse (2.4 standard errors from the Hill estimator). Lower insets demonstrate an enclave (solid line) and its surrounding cluster (dashed line). In the upper inset, the enclave is absorbed into its surrounding cluster. (d) Clusters' structure at the critical point of the NEP model (RP model with absorbed enclaves). The absorption of enclaves is implemented by identifying the longest boundary of each cluster and absorbing all the nodes within this boundary in the cluster (see Supplemental Material [6] for more details).

protocol). This is illustrated in the insets to Figs. 1(c) and 2(a) and in the Supplemental Material [6]. As we show, our NEP model exhibits mixed properties of both discontinuous and continuous phase transitions, including the anomalous critical behavior, consistent with the experiments.

In the 2D random percolation model, close to the percolation transition point,  $p = p_c$ , the strength (i.e., fraction of total mass) of the cluster with the largest mass scales as  $P \sim |\Delta p|^{\beta'}$ , where  $\Delta p = p - p_c$ .  $P$  vanishes at the critical point in the thermodynamic limit, such that the largest cluster mass scales as  $M^{d_f/d}$ . In the following,

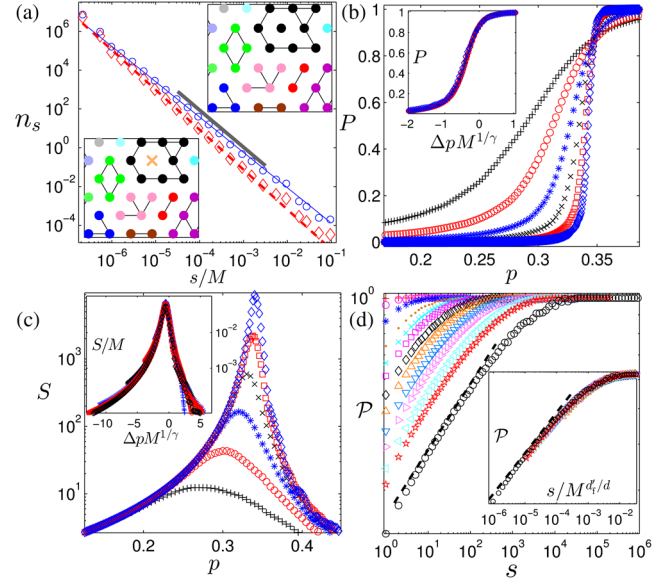


FIG. 2 (color online). (a) Cluster mass distribution at the percolation transition of the RP (diamonds) and NEP (circles) models, with  $M = 2000^2$ . The long lines indicate power laws with  $\tau' = 187/91$  (dashed line) and  $\tau = 1.82$  (solid line) [Eq. (9)]. The short line indicates the experimental  $\tau \approx 1.91$  observed over 2 decades. Insets illustrate cluster structures of the RP (left inset) and NEP models (right inset) on a triangular lattice for  $0 < p < 1$  (see Supplemental Material [6] for  $p = 0, 1$  cases). Colors (online) represent different clusters. The cross in the left inset indicates an enclave that is absorbed in the NEP model (right inset). The absorption of enclaves in the NEP model changes the distribution of clusters sizes and can account for the experimental observation of  $\tau < 2$  in Ref. [5]. (b) Demonstration of the discontinuous transition in the NEP model. Strength of the largest cluster,  $P$ , as a function of bond density,  $p$  for different system sizes, from  $M = 12$  to 400. Inset: collapse of the data from the main figure using Eq. (4) and  $\gamma = 8/3$ . (c) Demonstration of the critical transition in the NEP model. Average cluster,  $S$ , as a function of bonds density,  $p$  for the same system sizes as in (b). Inset: collapse of the data from the main figure using Eq. (6) and  $\gamma = 8/3$ . (d) Probability of an  $s$  cluster to be not an enclave of another cluster,  $\mathcal{P}$ , at the percolation transition of the RP model for different system sizes, from  $M = 6$  to 2000. Inset: collapse of the data from the main figure using Eq. (7). The dashed lines indicate power law  $a = 0.1706$  obtained from Eqs. (8) and (9).

we denote by primed symbols the quantities for the RP model and reserve unprimed symbols for the NEP model. The transition in the RP model is critical, such that the correlation length diverges as  $\xi \sim |\Delta p|^{-\nu'}$ , with  $\nu' = 4/3$  [8,9]. The cluster masses are distributed as a power law with a Fisher exponent  $\tau' = 187/91 > 2$ :  $n'_s \sim Ms^{-\tau'}$ , where  $n'_s$  is the number of clusters with mass  $s$  [see Fig. 2(a)]. The Fisher exponent is related to the fractal dimension by the hyperscaling relation,  $\tau' = d/d'_f + 1$ . Therefore, the continuity of the transition in an RP model follows from  $d'_f < d$  or, equivalently, from  $\tau' > 2$ . Thus, the qualitative form of the percolation transition is

reflected in the value of the Fisher exponent and fractal dimension [7].

In contrast, the absorption of enclaves in the NEP model leads to a different universality class, although the critical value  $p_c$  remains the same, since enclaves do not themselves percolate. Moreover, because enclaves are wholly surrounded by another cluster, the absorption of enclaves does not change the scaling of the radius of gyration of clusters. Thus, the divergence of the correlation length is as in the RP model, with  $\nu = \nu'$ . After absorption of enclaves, the surviving compact clusters are Euclidean with  $d_f = d = 2$ .

The transition in the NEP model is still critical, since the correlation length diverges there. Therefore, the distribution of cluster masses is scale free at the transition. The mass of the largest cluster below the transition point,  $p < p_c$ , scales as  $\xi^d$ , such that it remains finite in the thermodynamic limit,  $M \rightarrow \infty$ . At the transition point, where  $\xi \sim M^{1/d}$ , the mass of the largest cluster scales as  $M$ . Thus, the strength of the largest cluster in the thermodynamic limit exhibits a discontinuous jump from 0 for  $p < p_c$  to a positive value at  $p = p_c$ . The only possibility for getting both the discontinuity and the criticality at the transition point is that the number of clusters with mass  $s$  is sublinear with the system size and is given by

$$n_s \sim M^{\tau-1} s^{-\tau}, \quad (1)$$

with Fisher exponent  $\tau < 2$ . Only, in this case, the critical, power-law distribution possesses a sufficiently heavy tail such that the mass of the largest cluster scales as the total mass, providing both criticality and discontinuity (see Refs. [11–14] and Supplemental Material [6]). Other exceptions to the usual second-order nature of percolation transition include interdependent networks [15,16], hierarchical structures [17], which can exhibit discontinuous transitions between the two phases. The possibility of such first-order-like percolation transitions in simple networks has been the subject of considerable recent debate. Starting from the explosive percolation [18], this and other models have been analyzed to show sharp transitions [12,14,19–26], which, in some cases, nevertheless, become continuous in the thermodynamic limit. Mixed phase transitions were found for several update percolation procedures [27]. In some cases the transition is at the point  $p_c = 1$  (see, e.g., Ref. [28]) while in other cases it is for  $p_c < 1$  (like in the NEP model and, e.g., Ref. [29]). Also, bootstrap percolation models have been found to exhibit discontinuous phase transitions, although it remains unclear whether these are critical in 2D [30–32]. Beyond percolation, similar issues arise, e.g., in thermal systems [33–35] and in the jamming transition, for which several phase-defining quantities or order parameters are possible. Interestingly, some of these exhibit discontinuous behavior, while others are continuous [36].

The upper bound of 2 for the Fisher exponent in the NEP model can be obtained analytically. To do so, consider the scaling of number of clusters possessing mass  $s$  at the transition point,  $n_s(p = p_c)$ . A cluster in the NEP model with no enclaves is Euclidean in contrast to the RP model where clusters possess fractal dimension  $d'_f$ . Therefore, one can relate  $n_s$  and the same quantity of the RP model,  $n'_s$ , using

$$n_s \sim n'_s \mathcal{P}(s') \frac{ds'}{ds} \sim M s^{-2} \mathcal{P}(s'). \quad (2)$$

Here  $s'$  is  $s^{d'_f/d}$  and  $\mathcal{P}(s)$  is the probability that a cluster with mass  $s$  is not an enclave in the RP model. The last equality in Eq. (2) follows from the hyperscaling relation of  $\tau'$  and  $d'_f$ . Smaller clusters are expected to have a higher probability to be an enclave and, therefore, to be absorbed in their surrounding clusters during the elimination of enclaves. Thus,  $\mathcal{P}(s)$  monotonically increases with  $s$ . This implies an upper bound for the Fisher exponent of the NEP model,  $\tau < 2$ , in agreement with the experiment. For such a heavy tail distribution of cluster masses the total number of clusters,  $n$ , is not an extensive quantity. Integrating Eq. (1), one obtains

$$n \sim M^{\tau-1}. \quad (3)$$

In the NEP model, the size of the jump of  $P$  at the transition and the scaling ansatz for  $P$  can now be obtained using Eq. (1) with  $\tau < 2$ . For  $p > p_c$ , the largest cluster has a mass that scales as  $M$ . The remaining mass of all the other clusters combined scales sublinearly with  $M$ , as  $\int^{\xi^2} n_s s ds \sim M^{\tau-1} \xi^{4-2\tau}$ . Thus, the strength of the largest cluster is 1 above the transition in the thermodynamic limit. In this limit, the discontinuity of  $P$  in the NEP model is from 0 to 1 at  $p = p_c$ . The finite-size scaling ansatz for the largest cluster strength is given by (see Supplemental Material [6])

$$P = \mathcal{G}(\Delta p M^{1/\gamma}), \quad (4)$$

where  $\mathcal{G}(-\infty) = 0$  and  $\mathcal{G}(\infty) = \Delta P = 1$ .

One can calculate other critical exponents of the NEP model in the following way. Since all the clusters are Euclidean,  $d_f = d = 2$ , the cutoff of the  $n_s$  power-law distribution is  $\chi \sim \xi^d \sim |\Delta p|^{-d\nu}$ , such that  $\sigma = 1/d\nu = \frac{3}{8}$ , since  $\chi \sim |\Delta p|^{-1/\sigma}$ . For  $\tau < 2$ , the average cluster size,

$$S = \frac{1}{M} \sum_{s=1}^{\infty} n_s s^2, \quad (5)$$

scales as the cutoff,  $\chi$ , such that  $\gamma = 1/\sigma = \frac{8}{3}$ , since  $S \sim |\Delta p|^{-\gamma}$ . The prime in Eq. (5) indicates that the sum runs over all nonpercolating clusters. We expect the

following scaling ansatz for the average cluster mass (see Supplemental Material [6]):

$$S = M\mathcal{H}(\Delta p M^{1/\gamma}). \quad (6)$$

The quantity  $S$  in Eq. (5) is analogous to the susceptibility in thermal systems, where the diverging susceptibility is a signature of a second-order phase transition. In the NEP model, the divergence of  $S$  comes along with a discontinuity of  $P$ —a signature of the first-order-like phase transition. Therefore, the critical exponent  $\beta$  and the conductivity exponent  $\mu$  are both zero, such that the usual scaling law  $\gamma + 2\beta = d\nu$  remains valid.

As one can see from Eqs. (1) and (2), the actual value of the Fisher exponent is determined by the functional dependence of  $\mathcal{P}(s)$ . Since the only relevant mass scale at the transition point of the RP model is  $M^{d_f/d}$ ,

$$\mathcal{P}(s) = \mathcal{F}\left(\frac{s}{M^{d_f/d}}\right) \sim \left(\frac{s}{M^{d_f/d}}\right)^a, \quad (7)$$

where  $\mathcal{F}$  is a scaling function and [after combining Eqs. (1), (2), and (7)]

$$a = (2 - \tau) \frac{d}{d_f}. \quad (8)$$

Other properties of the NEP model are derived and summarized in the Supplemental Material [6].

*Numerical analysis.*—To verify our theoretical analysis of the NEP model, we simulate it on a 2D triangular lattice (see details in the Supplemental Material [6]), where a random occupation of bonds results in a continuous, second-order-like, transition when the probability of a bond to be occupied is  $p = p_c = 2 \sin(\pi/18)$  [37]. For the NEP model, we first demonstrate the discontinuous transition behavior of  $P$ . As shown in Fig. 2(b), the transition of  $P$  from 0 to 1 as a function of  $p$  becomes steeper with increasing system size,  $M$ . In fact, as shown in the inset of Fig. 2(b), one can collapse the data from Fig. 2 using the scaling form (4) with the calculated value of  $\gamma = 8/3$ . Therefore, in the limit  $M \rightarrow \infty$  at  $p = p_c$  the value of  $P$  discontinuously jumps from 0 to 1.

To demonstrate criticality in the NEP model, we perform finite-size analysis of the average, nonpercolating cluster size—the analogue of the susceptibility in thermal systems, plotting  $S$  vs  $p$  for different values of the total mass of the system,  $M$ . In Fig. 2(c) one can see that the peak value of  $S$  depends on the system size. In fact, as shown in the inset of Fig. 2(c), one can collapse the data from Fig. 2(c) using the scaling form (6) with the calculated value of  $\gamma = 8/3$ . Therefore, in the limit  $M \rightarrow \infty$ ,  $S$  diverges at the transition, as in a second-order phase transition. Thus, our finite-size scaling analysis confirms the hybrid nature of the phase transition in the NEP model, with discontinuity in the order

parameter,  $P$ , and yet divergence of the susceptibility,  $S$ , in the thermodynamic limit.

As is mentioned above, such a hybrid phase transition can exist only if the Fisher exponent is smaller than its upper bound of 2. As one can see in Fig. 2(a), the cluster mass distribution is consistent with Eq. (1) with

$$\tau = 1.82 \pm 0.01 < 2, \quad (9)$$

in agreement with the considerations above. The above estimation of  $\tau$  in Eq. (9) was obtained using Eq. (3) (see details in the Supplemental Material [6]). The obtained value of  $\tau$  is in agreement with our experimental results [see Fig. 1(c)].

The difference of  $\tau$  from 2 is due to a power-law scaling of the  $\mathcal{P}(s) \sim (s/M^{d_f/d})^a$ , as indicated in Eq. (8). To verify this, we calculated numerically the probability of an  $s$  cluster in the RP model to not be an enclave for different systems sizes,  $M$ . As shown in Fig. 2(d), the dependence is consistent with Eqs. (7), (8), and (9). Moreover, all the  $\mathcal{P}(s)$  data, for different  $M$  values, collapse to a master curve with a power-law dependence on  $s/M^{d_f/d}$ , confirming Eq. (7) [see inset of Fig. 2(d)]. With this, we complete the numerical validation of the analytical arguments.

We have shown that a simple extension of the RP model, with absorbed enclaves, exhibits, simultaneously, features of both discontinuous and continuous phase transitions. This model is in a distinct universality class from the RP model, with different critical exponents for all but the correlation length. Importantly, motor activated gels appear to constitute an experimental realization of this universality class.

This work was supported by the Foundation for Fundamental Research on Matter (FOM), which is part of the Netherlands Organisation for Scientific Research (NWO), and by a VIDI grant from NWO (GK).

- 
- [1] M. Sahimi, *Applications of Percolation Theory* (CRC Press, London, 1994).
  - [2] P.-G. de Gennes, *Scaling Concepts in Polymer Physics* (Cornell University Press, Ithaca, 1979).
  - [3] C. P. Broedersz and F. C. MacKintosh, *Rev. Mod. Phys.* **86**, 995 (2014).
  - [4] J. Nagler, A. Levina, and M. Timme, *Nat. Phys.* **7**, 265 (2011).
  - [5] J. Alvarado, M. Sheinman, A. Sharma, F. C. MacKintosh, and G. H. Koenderink, *Nat. Phys.* **9**, 591 (2013).
  - [6] See Supplemental Material at <http://link.aps.org/supplemental/10.1103/PhysRevLett.114.098104> for more details.
  - [7] D. Stauffer and A. Aharony, *Introduction To Percolation Theory* (Taylor & Francis, London, 1994).
  - [8] M. Den Nijs, *J. Phys. A* **12**, 1857 (1979).
  - [9] B. Nienhuis, *Phys. Rev. Lett.* **49**, 1062 (1982).
  - [10] A. Clauset, C. Rohilla Shalizi, and M. E. J. Newman, *SIAM Rev.* **51**, 661 (2009).

- [11] E. J. Friedman and A. S. Landsberg, *Phys. Rev. Lett.* **103**, 255701 (2009).
- [12] R. A. da Costa, S. N. Dorogovtsev, A. V. Goltsev, and J. F. F. Mendes, *Phys. Rev. Lett.* **105**, 255701 (2010).
- [13] H. Hooyberghs and B. Van Schaeuybroeck, *Phys. Rev. E* **83**, 032101 (2011).
- [14] R. A. da Costa, S. N. Dorogovtsev, A. V. Goltsev, and J. F. F. Mendes, *Phys. Rev. E* **89**, 042148 (2014).
- [15] S. V. Buldyrev, R. Parshani, G. Paul, H. E. Stanley, and S. Havlin, *Nature (London)* **464**, 1025 (2010).
- [16] J. Gao, S. V. Buldyrev, H. E. Stanley, and S. Havlin, *Nat. Phys.* **8**, 40 (2011).
- [17] S. Boettcher, V. Singh, and R. M. Ziff, *Nat. Commun.* **3**, 787 (2012).
- [18] D. Achlioptas, R. M. D'Souza, and J. Spencer, *Science* **323**, 1453 (2009).
- [19] A. A. Moreira, E. A. Oliveira, S. D. S. Reis, H. J. Herrmann, and J. S. Andrade, *Phys. Rev. E* **81**, 040101 (2010).
- [20] Y. S. Cho, B. Kahng, and D. Kim, *Phys. Rev. E* **81**, 030103 (2010).
- [21] R. M. D'Souza and M. Mitzenmacher, *Phys. Rev. Lett.* **104**, 195702 (2010).
- [22] F. Radicchi and S. Fortunato, *Phys. Rev. E* **81**, 036110 (2010).
- [23] N. A. M. Araújo and H. J. Herrmann, *Phys. Rev. Lett.* **105**, 035701 (2010).
- [24] O. Riordan and L. Warnke, *Science* **333**, 322 (2011).
- [25] J. Nagler, T. Tiessen, and H. W. Gutch, *Phys. Rev. X* **2**, 031009 (2012).
- [26] R. A. da Costa, S. N. Dorogovtsev, A. V. Goltsev, and J. F. F. Mendes, *Phys. Rev. E* **90**, 022145 (2014).
- [27] N. A. M. Araújo, J. S. Andrade, R. M. Ziff, and H. J. Herrmann, *Phys. Rev. Lett.* **106**, 095703 (2011).
- [28] Y. S. Cho, S. Hwang, H. J. Herrmann, and B. Kahng, *Science* **339**, 1185 (2013).
- [29] M. Schröder, S. E. Rahbari, and J. Nagler, *Nat. Commun.* **4** (2013).
- [30] J. Chalupa, P. L. Leath, and G. R. Reich, *J. Phys. C* **12**, L31 (1979).
- [31] J. Schwarz, A. J. Liu, and L. Chayes, *Europhys. Lett.* **73**, 560 (2006).
- [32] H. Chae, S.-H. Yook, and Y. Kim, *Phys. Rev. E* **89**, 052134 (2014).
- [33] D. J. Thouless, *Phys. Rev.* **187**, 732 (1969).
- [34] Y. Kafri, D. Mukamel, and L. Peliti, *Phys. Rev. Lett.* **85**, 4988 (2000).
- [35] A. Bar and D. Mukamel, *Phys. Rev. Lett.* **112**, 015701 (2014).
- [36] M. Van Hecke, *J. Phys. Condens. Matter* **22**, 033101 (2010).
- [37] I. W. Essam, D. S. Gaunt, and A. J. Guttmann, *J. Phys. A* **11**, 1983 (1978).